

# On-Chip Characterization of High-Loss Liquids between 750 GHz and 1100 GHz

Juan Cabello-Sánchez, *Student Member, IEEE*, Vladimir Drakinskiy, Jan Stake, *Senior Member, IEEE*,  
Helena Rodilla, *Senior Member, IEEE*

**Abstract**—Terahertz spectroscopy is a promising tool for analyzing the picosecond dynamics of biomolecules, which is influenced by surrounding water molecules. However, water causes extreme losses to terahertz signals, preventing sensitive measurements at this frequency range. Here, we present sensitive on-chip terahertz spectroscopy of highly lossy aqueous solutions using a vector network analyzer, contact probes, and a coplanar waveguide with a 0.1 mm wide microfluidic channel. The complex permittivities of various deionized water/isopropyl alcohol concentration are extracted from a known reference measurement across the frequency range 750–1100 GHz and agrees well with literature data. The results prove the presented method as a high-sensitive approach for on-chip terahertz spectroscopy of high-loss liquids, capable of resolving the permittivity of water.

**Index Terms**—Coplanar waveguides, isopropyl alcohol, material properties, microfluidic channels, on-wafer measurements, permittivity, scattering parameters, terahertz spectroscopy, vector network analyzers, water

## I. INTRODUCTION

**T**erahertz (THz) spectroscopy is an indispensable tool to analyze light-weight molecules with applications in astronomy and chemistry. With new technological developments, the application of THz technology has extended to fields as diverse as security [1], communications [2], pharmaceutical control [3], medicine and biology [4]. In biology, THz waves have shown to be a relevant method for studying picosecond dynamics of biomolecules [5], [6], predicted to be key for their biological function [7] in which water plays an important role [8]. Aqueous samples have been measured with time-domain spectroscopy (TDS), one of the most common THz spectroscopy methods, with free-space transmission [9], free-space reflection [10], and on-chip setups [11], [12]. However, despite having a relatively high dynamic range, necessary for measuring high-loss samples, the low time-averaged power and wide bandwidth typically yield measurements with a low signal-to-noise ratio (SNR), limiting the smallest detectable signal change [13]. The low SNR further plummets when measuring high-loss aqueous samples (around 100 dB/mm [9]) in higher-loss chip setups, hindering pure water measurements at frequencies above 0.5 THz [12], or having to avoid liquid

sample in the region with the most intense electric field to minimize losses [11], [14], but sacrificing sensitivity.

A promising method for obtaining high SNR for on-chip applications is measuring S-parameters using vector network analyzers (VNA), a common measuring method at microwave and millimeter-wave frequencies. This method is based on an electronic heterodyne technique, and benefits from having first-class frequency resolution ( $\sim 1$  Hz), about 20 dB higher dynamic range than TDS systems at 1 THz [15], traceability to the International System of Units [16], and can use calibration techniques to move the reference plane to the region of interest [17]; whereas the downside is that the bandwidth is limited to a waveguide band. The frequency range of VNA measurements applied to biology has been typically restricted to microwave [18] and millimeter-wave frequencies [19], [20]. However, recent development in heterodyne technology has increased the maximum frequency of VNA analysis up to 1.5 THz [21] in rectangular waveguides, and up to 1.1 THz for on-chip measurements using contact probes [22]. Contact probes offer an efficient way to guide the generated power directly into the sensing chip (compared to free-space coupling), thus increasing the sensibility of the method.

In this letter, we demonstrate the use of a vector network analyzer and contact probes for THz spectroscopy of high-loss aqueous samples contained in a chip. We describe the design of the low-loss sensing waveguide and its fabrication, the measurement setup, and how the complex refractive index was extracted from the measured complex transmission coefficient. This is a first step towards a miniaturized chip sensor for high-loss liquid samples at THz frequencies.

## II. METHOD

For sensing liquid samples on a chip, we used a coplanar waveguide (CPW) [23], which provides easy interfacing with ground-signal-ground probes (Fig. 1.a). The CPW was designed to suit both the measurement probe's pitch (25  $\mu\text{m}$ ) and characteristic impedance (50  $\Omega$ ) [22], yielding a central strip width of 23.5  $\mu\text{m}$  and a ground separation of 1.5  $\mu\text{m}$ . The CPW was designed on a ultra-thin 23  $\mu\text{m}$  thick polyethylene terephthalate (PET) film substrate ( $\epsilon' = 3.15$  and  $\tan(\delta) = 0.017$  at 1 THz [24]), to avoid power leakage [25] to undesirable substrate modes [26]. The CPWs and their dedicated calibration standards were fabricated using e-beam lithography and evaporation of 20 nm Ti and 350 nm Au on top of the PET substrate.

The PET substrate containing the CPWs is held on top of a polyethylene supporting substrate to avoid coupling with

This work was supported by the Swedish Research Council (Vetenskapsrådet) and Knut and Alice Wallenberg Foundation.

Juan Cabello-Sánchez, Vladimir Drakinskiy, Jan Stake and Helena Rodilla are with the Terahertz and Millimetre Wave Laboratory, Chalmers University of Technology, SE-412 96 Gothenburg, Sweden. (e-mail: juan-cab@chalmers.se; vladimir.drakinskiy@chalmers.se; jan.stake@chalmers.se; rodilla@chalmers.se)

Manuscript received July 17, 2020; revised ..., 2020.

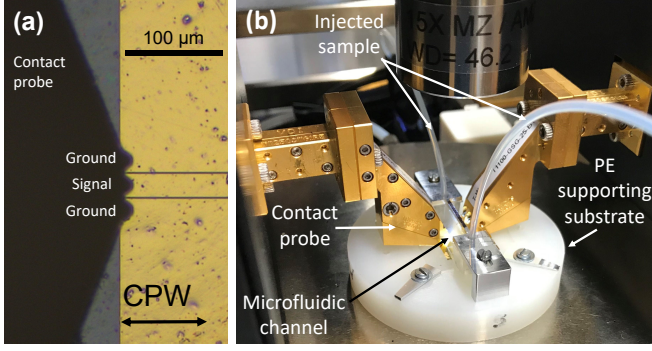


Fig. 1. (a) Micrograph of the CPW being excited by the ground-signal-ground probe. (b) Photograph of measurement setup during measurements.

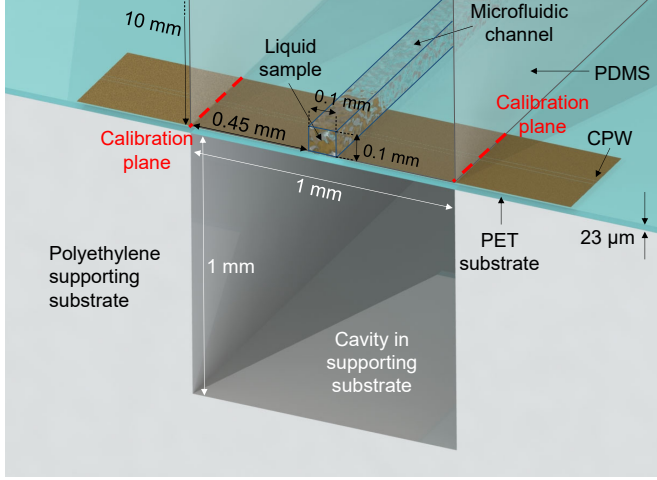


Fig. 2. Illustration of the cross-section of the microfluidic channel filled with sample intersecting the CPW.

the probe station's metal chuck during the measurements (Fig. 1.b). The polyethylene supporting substrate had a 1 mm deep and 1 mm long air cavity under the measured CPW, suspending it on air (Fig. 2). On top of the PET substrate, an interchangeable polydimethylsiloxane (PDMS) microfluidic channel was clamped to the polyethylene supporting substrate. The microfluidic channel was designed to have a 100 μm wide square cross-section, whereas the cross-section of the PDMS containing the channel is 1 mm wide by 10 mm tall (Fig. 2). To deliver the sample into the microfluidic channel, input and output tubings were connected to the microfluidic channel.

We measured the complex transmission coefficient,  $\hat{T}_s$ , between 0.75 THz and 1.1 THz using a VNA Keysight N5242A connected to two VDI WR1.0SAX frequency extenders [27], having a typical/minimum dynamic range of 65/45 dB, respectively, and a continuous wave signal power higher than -40 dBm. To couple the signal to the sensing chip, we used DMPI T-Wave ground-signal-ground probes [22]. We used dedicated multi-line TRL [28] calibration structures to set the calibration plane at the air-PDMS interface (Fig. 2).

The aqueous samples consist of propan-2-ol (IPA) in deionized-water (DI-H<sub>2</sub>O) with different concentrations—0, 10, 20, 30, 40, and 50% of IPA in volume. The samples were pumped into the microfluidic channel from higher to

lower concentration of IPA through the input tube using a syringe and flushing air between samples. The pressure was adjusted to atmospheric pressure by removing the syringe momentarily after introducing each sample. The probes were kept in contact with the chip throughout all measurements to minimize probing position uncertainty. Each sample was measured five times in consecutive VNA sweeps with an intermediate frequency bandwidth of 50 Hz.

The effective refractive index of the sample-loaded CPW ( $\hat{n}_e = n_e - j\kappa_e$ ) was calculated by comparing the measured transmission with a reference measurement,  $\hat{T}_r$  (average of five measurements with DI-water as sample), following the equation:

$$\hat{n}_e = \hat{n}_r - \frac{\ln [\hat{T}_s / \hat{T}_r]}{jk_0 l_s} \quad (1)$$

where  $k_0$  is the vacuum wavenumber,  $l_s$  is the effective sample length, and  $\hat{n}_r$  is the effective refractive index of the reference.  $\hat{n}_r$  was obtained from analytical expressions for multilayered substrates on CPWs [29] and using a double Debye model for water [9] in order to include the frequency-dependent permittivity.

Finally, the sample's refractive index  $\hat{n}_s$  was found from measured CPW's effective refractive index,  $\hat{n}_e$ , by using the same analytical expressions for multilayered substrates on CPWs [29]. According to it, the equation relating the sample permittivity with the CPW's effective permittivity is:

$$\hat{n}_e^2 = \hat{\epsilon}_e = 1 + \frac{1}{2}(\hat{n}_s^2 - 1) \frac{K(k)K(k'_s)}{K(k')K(k_s)} + \frac{1}{2}(\hat{n}_{sub}^2 - 1) \frac{K(k)K(k'_{sub})}{K(k')K(k_{sub})} \quad (2)$$

where  $K$  is the complete elliptical integral of the first kind, and  $k, k', k_s, k'_s, k_{sub}, k'_{sub}$ , are terms depending on the geometry of the CPW cross-section, superstrate (sample) and substrate, respectively [29]. The analytical expression (eq. 2) agrees well with more detailed 3D electromagnetic simulations of the multilayered CPW.

### III. RESULTS

We measured the transmission of a 1 mm long CPW with the PDMS microfluidic channel containing IPA/DI water solutions from 0.75 THz to 1.1 THz. For DI-water, the typical insertion loss was in the order of 25 dB. Fig. 3a-b shows the phase and magnitude, respectively, of the transmission for each sample normalized to the reference measurement (DI-water). Solid lines represent the average of five successive measurements, whereas the shadows represent their standard deviation. Both the normalized magnitude and phase consistently decrease for increasing IPA concentration, as expected from literature values [9], [30]. The artifacts observed around 0.95 THz and 1 THz, which appear as resonances in both magnitude and phase of the transmission, were also observed without any microfluidic channel. A possible explanation is parasitic probe-to-probe coupling effects or calibration artifacts [31]. The measurements' noise increases noticeably after 1.05 THz due to a drop in the dynamic range at the end of the frequency

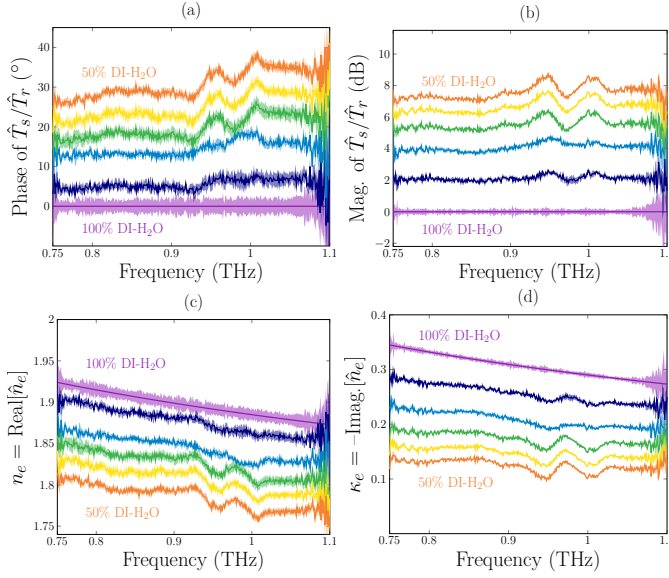


Fig. 3. Transmission measurements can resolve magnitude and phase differences between high-loss aqueous samples. Transmission (a) phase difference, and (b) power ratio with respect to reference measurement for the IPA/DI-H<sub>2</sub>O samples (from 50% to 100% DI-H<sub>2</sub>O in steps of 10%). (c) Real and (d) imaginary part of effective refractive indices of the CPW with samples. Lines indicate the mean of five measurements, whereas shadows indicate the standard deviation.

extender band. The relative error shows to be smaller for  $\kappa_e$  than for  $n_e$ , implying that in this case, smaller sample changes can be detected with attenuation measurements than with phase measurements. For water measurements the SNR was typically higher than 25 dB.

The real and imaginary effective refractive indices are shown in Fig. 3.c-d, where all high-loss samples have been successfully resolved. A relatively large effective length  $l_s = 250 \mu\text{m}$  was used since part of the liquid was found to extend between the PDMS and CPW substrate. Fig. 4 shows the samples' extracted real and imaginary permittivities at 0.8 THz versus sample DI-water concentration, showing error bars with 95% confidence interval. Both the real and imaginary parts of the permittivities change consistently with the changes of IPA concentration. The analytically extracted sample permittivities are also plotted with the permittivity of the IPA/water mixtures using literature values, using a modified Bruggeman's approximation for binary mixtures of polar liquids [32], with equation:

$$\left[ \frac{\epsilon_m - \epsilon_{H_2O}}{\epsilon_{IPA} - \epsilon_{H_2O}} \right] \left[ \frac{\epsilon_{IPA}}{\epsilon_m} \right]^{1/3} = 1 - \left[ a - (a-1)\alpha_{H_2O} \right] \alpha_{H_2O} \quad (3)$$

where  $\epsilon_{H_2O}$  and  $\epsilon_{IPA}$  are literature values of the permittivities of water [9] and IPA [30] respectively,  $\alpha_{H_2O}$  is the volume concentration of water,  $\epsilon_m$  the permittivity of the mixture, and  $a = 1.33$  is the fitting factor for propanol-water samples [32].

#### IV. CONCLUSION

This letter presents an on-chip dielectric spectroscopy method capable of measuring high-loss aqueous samples enabled by VNA and ground-signal-ground probes. Similar

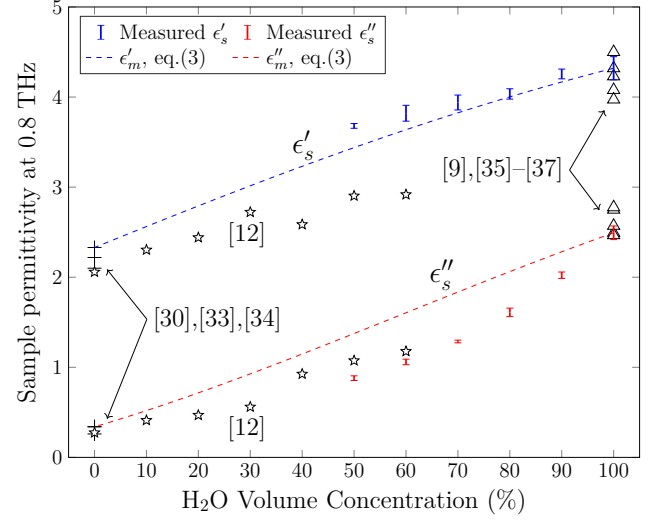


Fig. 4. Obtained sample permittivities show consistent change with varying water concentration. Permittivity of IPA/DI-H<sub>2</sub>O samples vs. water concentration at 0.8 THz for this work (blue and red errorbars for 95% confidence interval) and literature values. Literature values of (+) IPA [30], [33], [34], ( $\Delta$ ) water [9], [35]–[37], and ( $\star$ ) IPA/H<sub>2</sub>O mixtures measured with a similar on-chip method [12] are plotted. The dashed lines show Bruggeman's model approximation for the change in water concentration, based in eq. (3).

attempts of broadband measurements of aqueous solutions with TDS had problems resolving the complex refractive index for high water content solutions at frequencies higher than 0.5 THz [12] or lost sensitivity from not placing sample where the sensor's field is strongest [11]. The main reasons why the presented method could measure aqueous samples sensitively is due to (1) a higher coupling efficiency when exciting the CPWs using the contact probes compared to other methods which couple a free-space beam into the substrate via an antenna; (2) the higher average power of continuous-wave THz signals produced by the VNA compared to other pulsed methods, like TDS; (3) a low-loss design of the CPW. The high dynamic range (typically 50 dB at calibration plane) allows to measure water with a sample length up to approximately 0.6 mm. Some drawbacks of this method are that (1) is limited to frequencies up to 1.1 THz, due to lack of contact probes at higher frequencies; (2) being limited to rectangular waveguide bands for a given setup, and (3) a higher cost. In perspective, this method is a first step towards a miniaturized system for sensing high-loss aqueous samples at THz frequencies, which could provide an integrated, accurate, and controlled platform to study fundamental biological phenomena in their native environment.

#### ACKNOWLEDGMENT

The authors would like to thank Mr. Mats Myremark for machining parts for the measurement setup and Dr. Kiryl Kustanovich for helping to fabricate the microfluidic channel. The devices were fabricated and measured in the Nanofabrication Laboratory and Kollberg Laboratory, respectively, at Chalmers University of Technology, Gothenburg, Sweden.

## REFERENCES

- [1] R. Appleby and R. N. Anderton, "Millimeter-wave and submillimeter-wave imaging for security and surveillance," *Proceedings of the IEEE*, vol. 95, no. 8, pp. 1683–1690, 2007, doi: 10.1109/JPROC.2007.898832.
- [2] H. J. Song and T. Nagatsuma, "Present and future of terahertz communications," *IEEE Transactions on Terahertz Science and Technology*, vol. 1, no. 1, pp. 256–263, 2011, doi: 10.1109/TTHZ.2011.2159552.
- [3] J. A. Zeitler, P. F. Taday, D. A. Newnham, M. Pepper, K. C. Gordon, and T. Rades, "Terahertz pulsed spectroscopy and imaging in the pharmaceutical setting - a review," *Journal of Pharmacy and Pharmacology*, vol. 59, no. 2, pp. 209–223, 2007, doi: 10.1211/jpp.59.2.0008.
- [4] E. Pickwell and V. P. Wallace, "Biomedical applications of terahertz technology," *Journal of Physics D: Applied Physics*, vol. 39, no. 17, 2006, doi: 10.1088/0022-3727/39/17/R01.
- [5] G. Aebas, K. A. Niessen, E. H. Snell, and A. G. Markelz, "Optical measurements of long-range protein vibrations," *Nature Communications*, vol. 5, pp. 1–7, 2014, doi: 10.1038/ncomms4076.
- [6] I. V. Lundholm, H. Rodilla, W. Y. Wahlgren, A. Duelli, G. Bourenkov, J. Vukusic, R. Friedman, J. Stake, T. Schneider, and G. Katona, "Terahertz radiation induces non-thermal structural changes associated with Fröhlich condensation in a protein crystal," *Structural Dynamics*, vol. 2, no. 5, 2015, doi: 10.1063/1.4931825.
- [7] K. Henzler-Wildman and D. Kern, "Dynamic personalities of proteins," *Nature*, vol. 450, no. 7172, pp. 964–972, 12 2007, doi: 10.1038/nature06522.
- [8] Y. Xu and M. Havenith, "Perspective: Watching low-frequency vibrations of water in biomolecular recognition by THz spectroscopy," *Journal of Chemical Physics*, vol. 143, no. 17, p. 224511, 2015, doi: 10.1063/1.4934504.
- [9] J. T. Kindt and C. A. Schmuttenmaer, "Far-Infrared Dielectric Properties of Polar Liquids Probed by Femtosecond Terahertz Pulse Spectroscopy," *The Journal of Physical Chemistry*, 1996, doi: 10.1021/jp960141g.
- [10] L. Thrane, R. H. Jacobsen, P. U. Jepsen, and S. R. Keiding, "THz reflection spectroscopy of liquid water," *Chemical Physics Letters*, vol. 240, no. 4, pp. 330–333, 1995, doi: 10.1016/0009-2614(95)00543-D.
- [11] J. Kitagawa, T. Ohkubo, M. Onuma, and Y. Kadoya, "THz spectroscopic characterization of biomolecule/water systems by compact sensor chips," *Applied Physics Letters*, vol. 89, no. 4, p. 41114, 2006, doi: 10.1063/1.2236295.
- [12] M. Swithenbank, A. D. Burnett, C. Russell, L. H. Li, A. G. Davies, E. H. Linfield, J. E. Cunningham, and C. D. Wood, "On-Chip Terahertz-Frequency Measurements of Liquids," *Analytical Chemistry*, vol. 89, no. 15, pp. 7981–7987, 8 2017, doi: 10.1021/acs.analchem.7b01235.
- [13] M. Naftaly and R. Dudley, "Methodologies for determining the dynamic ranges and signal-to-noise ratios of terahertz time-domain spectrometers," *Optics Letters*, vol. 34, no. 8, p. 1213, 4 2009, doi: 10.1364/ol.34.001213.
- [14] T. Ohkubo, M. Onuma, J. Kitagawa, and Y. Kadoya, "Micro-strip-line-based sensing chips for characterization of polar liquids in terahertz regime," *Applied Physics Letters*, vol. 88, no. 21, p. 212511, 5 2006, doi: 10.1063/1.2207989.
- [15] D. K. George, A. Charkhesht, and N. Q. Vinh, "New terahertz dielectric spectroscopy for the study of aqueous solutions," *Review of Scientific Instruments*, vol. 86, no. 12, p. 123105, 2015, doi: 10.1063/1.4936986.
- [16] N. M. Ridler and R. G. Clarke, "Establishing Traceability to the International System of Units for Scattering Parameter Measurements from 750 GHz to 1.1 THz," *IEEE Transactions on Terahertz Science and Technology*, vol. 6, no. 1, pp. 2–11, 2016, doi: 10.1109/TTHZ.2015.2502068.
- [17] R. F. Bauer and P. Penfield, "De-Embedding and Underterminating," *IEEE Transactions on Microwave Theory and Techniques*, vol. 22, no. 3, pp. 282–288, 1974, doi: 10.1109/TMTT.1974.1128212.
- [18] P. Velez, L. Su, K. Grenier, J. Mata-Contreras, D. Dubuc, and F. Martin, "Microwave Microfluidic Sensor Based on a Microstrip Splitter/Combiner Configuration and Split Ring Resonators (SRRs) for Dielectric Characterization of Liquids," *IEEE Sensors Journal*, vol. 17, no. 20, pp. 6589–6598, 2017, doi: 10.1109/JSEN.2017.2747764.
- [19] H. Rodilla, A. A. Kim, G. D. Jeffries, J. Vukusic, A. Jesorka, and J. Stake, "Millimeter-wave sensor based on a  $\lambda/2$ -line resonator for identification and dielectric characterization of non-ionic surfactants," *Scientific Reports*, vol. 6, no. October 2015, pp. 1–5, 2016, doi: 10.1038/srep19523.
- [20] X. Bao, I. Ocket, J. Bao, J. Doijen, J. Zheng, D. Kil, Z. Liu, B. Puers, D. Schreurs, and B. Nauwelaers, "Broadband Dielectric Spectroscopy of Cell Cultures," *IEEE Transactions on Microwave Theory and Techniques*, vol. 66, no. 12, pp. 5750–5759, 2018, doi: 10.1109/TMTT.2018.2873395.
- [21] D. Koller, S. Durant, C. Rowland, E. Bryerton, and J. Hesler, "Initial measurements with WM164 (1.1-1.5THz) VNA extenders," in *2016 41st International Conference on Infrared, Millimeter, and Terahertz Waves (IRMMW-THz)*, Copenhagen, 2016, pp. 1–2, doi: 10.1109/IRMMW-THz.2016.7758434.
- [22] M. F. Bauwens, N. Alijabbari, A. W. Lichtenberger, N. S. Barker, and R. M. Weikle, "A 1.1 THz micromachined on-wafer probe," in *2014 IEEE MTT-S International Microwave Symposium (IMS2014)*, Tampa, FL, 2014, pp. 1–4, doi: 10.1109/MWSYM.2014.6848607.
- [23] C. P. Wen, "Coplanar Waveguide: A Surface Strip Transmission Line Suitable for Nonreciprocal Gyromagnetic Device Applications," *IEEE Transactions on Microwave Theory and Techniques*, vol. 17, no. 12, pp. 1087–1090, 1969, doi: 10.1109/TMTT.1969.1127105.
- [24] N. Fuse, T. Takahashi, Y. Ohki, R. Sato, M. Mizuno, and K. Fukunaga, "Terahertz Spectroscopy as a New Tool for Insulating Material Analysis and Condition Monitoring," *IEEE Insulating Magazine*, vol. 27, no. 3, pp. 26–35, 2011, doi: 10.1109/MEI.2011.5871366.
- [25] J. Cabello-Sánchez, H. Rodilla, V. Drakinskiy, and J. Stake, "Transmission Loss in Coplanar Waveguide and Planar Goubau Line between 0.75 THz and 1.1 THz," in *2018 43rd International Conference on Infrared, Millimeter, and Terahertz Waves (IRMMW-THz)*, Nagoya, 2018, pp. 1–2, doi: 10.1109/IRMMW-THz.2018.8510326.
- [26] D. B. Rutledge, S. E. Schwarz, and A. T. Adams, "Infrared and submillimetre antennas," *Infrared Physics*, vol. 18, no. 5-6, pp. 713–729, 1978, doi: 10.1016/0020-0891(78)90094-5.
- [27] T. W. Crowe, B. Foley, S. Durant, K. Hui, Y. Duan, and J. L. Hesler, "VNA frequency extenders to 1.1 THz," in *2011 36th International Conference on Infrared, Millimeter, and Terahertz Waves (IRMMW-THz)*, Houston, TX, 2011, pp. 1–1, doi: 10.1109/irmmw-THz.2011.6105028.
- [28] R. B. Marks, "A Multiline Method of Network Analyzer Calibration," *IEEE Transactions on Microwave Theory and Techniques*, vol. 39, no. 7, pp. 1205–1215, 1991, doi: 10.1109/22.85388.
- [29] E. Chen and S. Y. Chou, "Characteristics of coplanar transmission lines on multilayer substrates: modeling and experiments," *IEEE Transactions on Microwave Theory and Techniques*, vol. 45, no. 6, pp. 939–945, 1997, doi: 10.1109/22.588606.
- [30] Y. Yomogida, Y. Sato, R. Nozaki, T. Mishina, and J. Nakahara, "Comparative study of boson peak in normal and secondary alcohols with terahertz time-domain spectroscopy," *Physica B: Condensed Matter*, vol. 405, no. 9, pp. 2208–2212, 2010, doi: 10.1016/j.physb.2010.02.010.
- [31] G. N. Phung, F. J. Schmuckle, R. Doerner, B. Kahne, T. Fritzsche, U. Arz, and W. Heinrich, "Influence of microwave probes on calibrated on-wafer measurements," *IEEE Transactions on Microwave Theory and Techniques*, vol. 67, no. 5, pp. 1892–1900, 2019, doi: 10.1109/TMTT.2019.2903400.
- [32] S. M. Puranik, A. C. Kumbharkhane, and S. C. Mehrotra, "The static permittivity of binary mixtures using an improved bruggeman model," *Journal of Molecular Liquids*, vol. 59, no. 2-3, pp. 173–177, 1994, doi: 10.1016/0167-7322(93)00665-6.
- [33] Y. Yomogida, Y. Sato, R. Nozaki, T. Mishina, and J. Nakahara, "Comparative dielectric study of monohydric alcohols with terahertz time-domain spectroscopy," *Journal of Molecular Structure*, vol. 981, no. 1-3, pp. 173–178, 2010, doi: 10.1016/j.molstruc.2010.08.002.
- [34] M. Swithenbank, C. Russell, A. D. Burnett, L. H. Li, A. G. Davies, E. H. Linfield, J. E. Cunningham, and C. D. Wood, "Accurate parameter extraction from liquids measured using on-chip terahertz spectroscopy," in *International Conference on Infrared, Millimeter, and Terahertz Waves, IRMMW-THz*, Copenhagen, 2016, pp. 1–2, doi: 10.1109/IRMMW-THz.2016.7758409.
- [35] P. U. Jepsen, U. Möller, and H. Merbold, "Investigation of aqueous alcohol and sugar solutions with reflection terahertz time-domain spectroscopy," *Optics Express*, vol. 15, no. 22, p. 14717, 2007, doi: 10.1364/OE.15.014717.
- [36] D. J. Segelstein, "The complex refractive index of water," Ph.D. dissertation, University of Missouri-Kansas City, 1981.
- [37] N. Q. Vinh, M. S. Sherwin, S. J. Allen, D. K. George, A. J. Rahmani, and K. W. Plaxco, "High-precision gigahertz-to-terahertz spectroscopy of aqueous salt solutions as a probe of the femtosecond-to-picosecond dynamics of liquid water," *Journal of Chemical Physics*, vol. 142, no. 16, p. 164502, 2015, doi: 10.1063/1.4918708.